

Astrophysical light scattering problems (PAP316)

Lecture 9a

Karri Muinonen

Academy Professor

Department of Physics, University of Helsinki, Finland

Icy moons of the outer planets, Contents

- Introduction
- Random and systematic errors of observations
- Jovian system: The Galilean moons
 - Summary of polarimetric observations
 - Phase-angle and longitude dependences of polarization for Callisto
 - Phase-angle and longitude dependences of polarization for Io, Europa, and Ganymede
 - Opposition effects for io, Europa, and Ganymede
 - Polarimetric data of Galilean moons from space probes
 - Spectral dependence of polarization for the Galilean moons
- Saturnian system: Enceladus, Dione, Rhea, Iapetus, and Tethys
 - Enceladus, Dione, Rhea, and Tethys
 - Iapetus
- Uranian system: Ariel, Umbriel, Titania, and Oberon
- Final notes on polarization of satellites
- Conclusion and perspectives

Introduction (1/2)

- Physical characterization of **astronomical objects** (e.g., surfaces of airless planetary objects)
- **Direct problem** of light scattering by particles with varying **particle size, shape, refractive index, and spatial distribution**
- **Inverse problem** based on **astronomical observations and/or experimental measurements**
- Plane of scattering, scattering angle, solar phase angle, degree of linear polarization

Introduction (2/2)

- Polarization opposition effect vs. brightness opposition effect (POE vs. BOE)
- Normal characteristics of coherent backscattering
- Shadow-hiding mechanism for BOE unable to explain negative polarization
- Near-field mechanism remains unestablished as an independent mechanism for polarization
- Phase angle vs. longitude dependence of polarization, challenging new aspect

Random and systematic errors of observations

- Random errors estimated by accounting for accumulated counts and sky background
- Systematic errors can rise even from bending of the telescope
- Systematic errors rise from the halo of the planet and from secondary incidence of light from the planet

Jovian system: The Galilean moons

- Mostly observed using ground-based telescopes
- Polarimetry at large phase angles obtained by the Galileo and Pioneer 11 missions
- Rotations locked into 1:1 resonance with the orbital motion about the planet (cf., the Moon)
- Entanglement of polarization dependences on phase angle and longitude

Phase-angle and longitude dependences of polarization for Callisto

- The two dependences cannot yet be well disentangled for Callisto
- Variations not due to observational errors!
- More observations needed

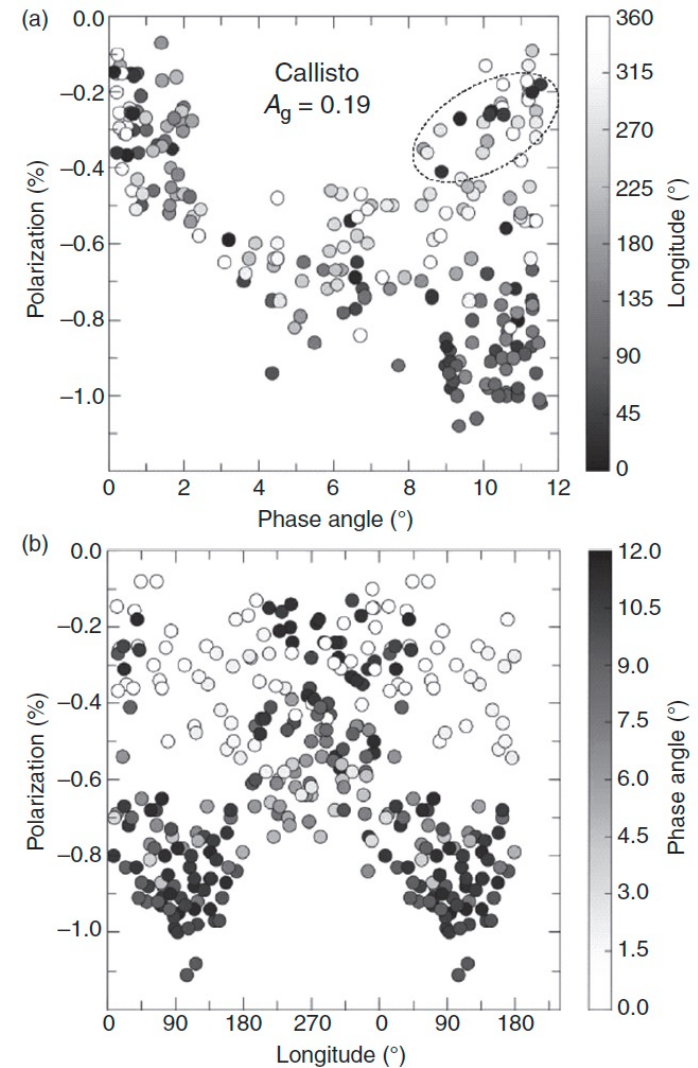


FIGURE 20.1 Measured degree of linear polarization for Callisto (V filter). (a) Phase angle plot: different longitudes are shaded according to the bar on the right-hand side of the figure; dashed ellipse shows a cluster of seven data points with very low (in absolute value) polarization for the leading hemisphere. (b) Longitude plot with shading according to phase angle. A one-and-a-half longitudinal cycle is plotted to provide overlap.

- Reduction to true longitude dependence with the help of fits using the trigonometric system for phase curves
- Example for phase angle of 6°

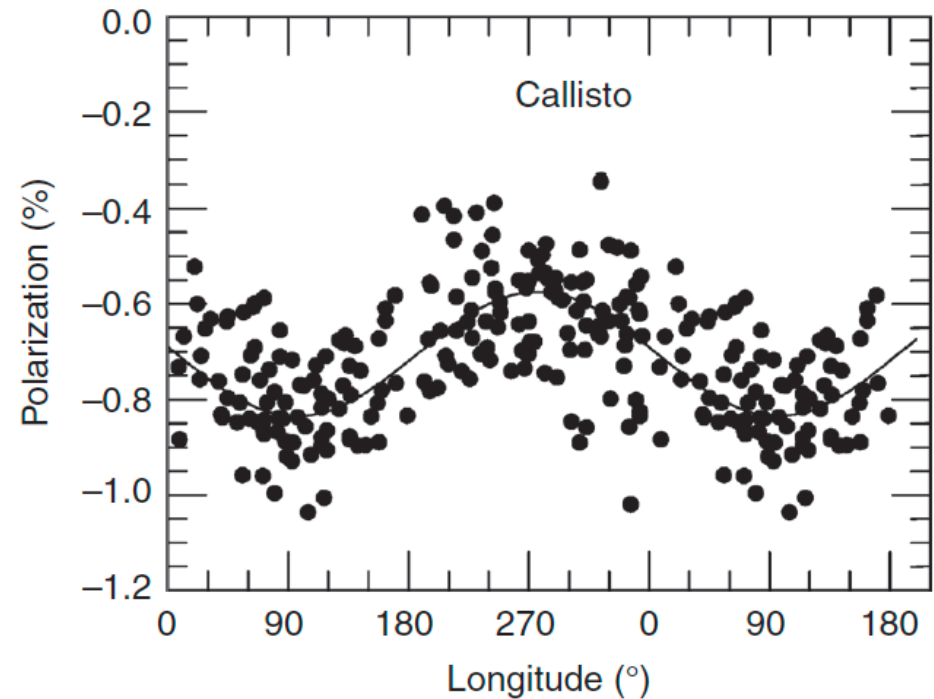


FIGURE 20.2 Longitude dependence of polarization for Callisto in the V filter at the phase angle $\alpha = 6^\circ$ after accounting for the phase-angle dependence of polarization in the first iteration.

- Polarization phase curves unveiled for leading and trailing hemispheres
- Significantly different polarization phase curves with lunar-like curve for the leading side
- Leading (trailing) side has a brightness opposition effect amplitude of 0.23-0.30 mag (0.15-0.18 mag)

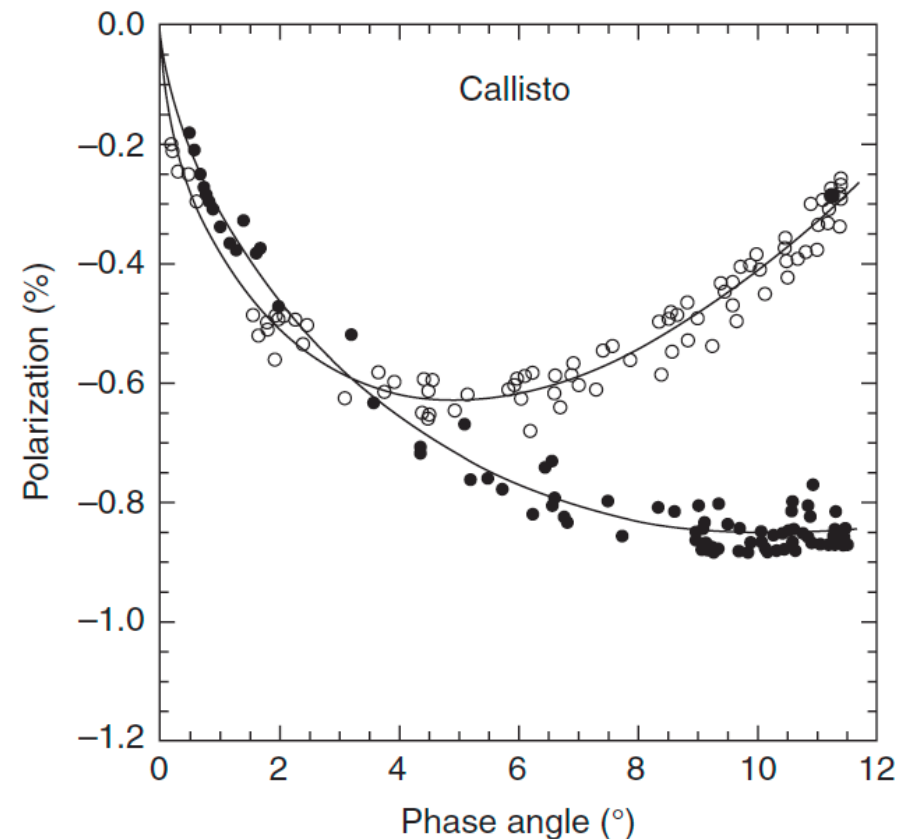


FIGURE 20.3 NPB for the leading (filled circles) and trailing (open circles) hemispheres of Callisto in the V filter after the correction for the orbital longitudinal variations (see Fig. 20.2). Solid curves represent the best fit to the data by a trigonometric expression of Lumme and Muinonen (1993).

Phase-angle and longitude dependences of polarization for Io, Europa, and Ganymede

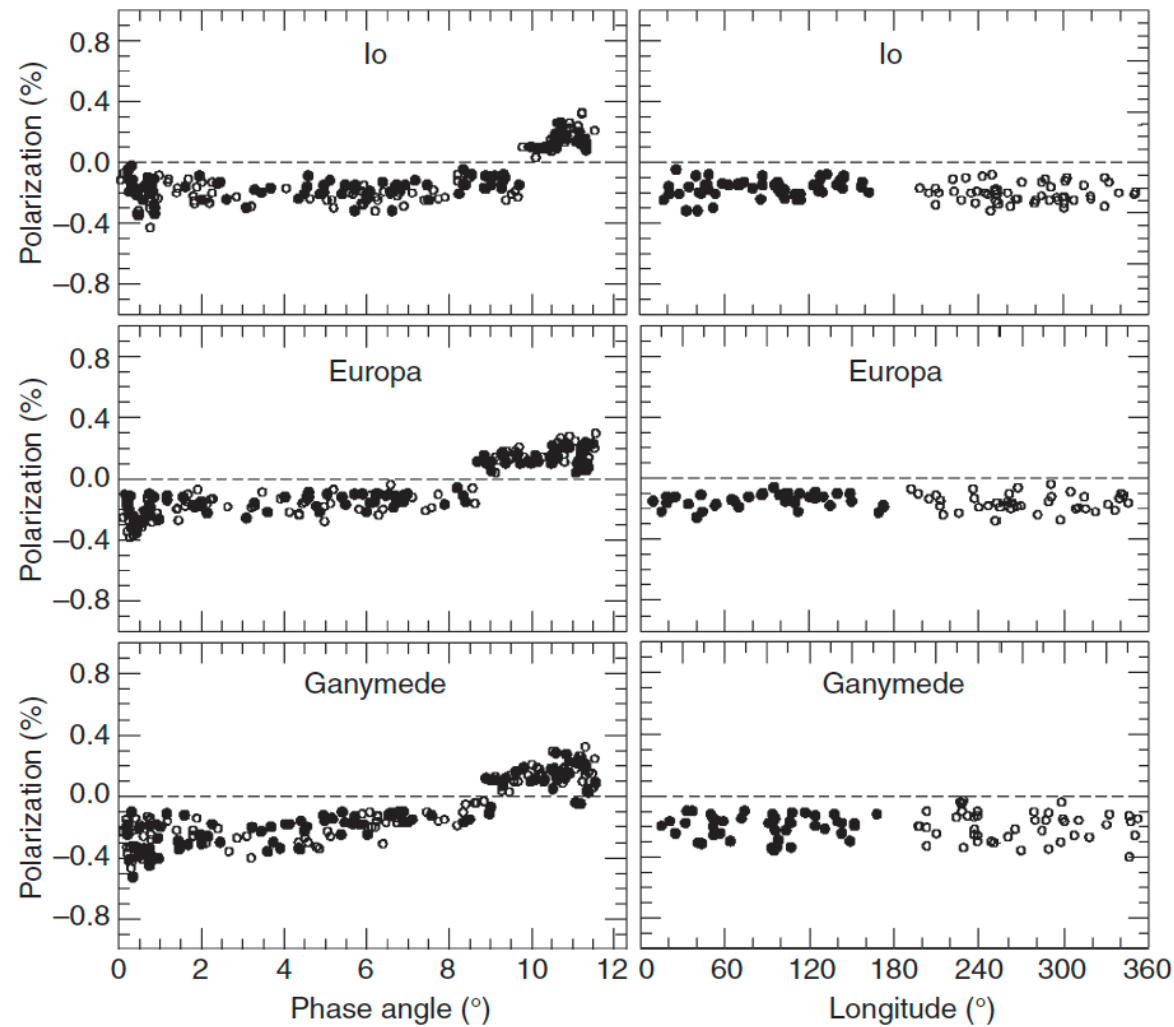


FIGURE 20.4 The observed degree of linear polarization versus phase angle (left panels) and longitude (right panels) for Io, Europa, and Ganymede. The filled (open) symbols show polarization for the leading (trailing) hemisphere. No attempt was made to separate phase angle and longitudinal dependence.

Opposition effects for Io, Europa, and Ganymede

- Sharp brightness opposition effects accompanied with polarization surges
- Pure coherent backscattering characteristics for positive single scattering polarization
- Europa flat negative polarization unseen in new observations

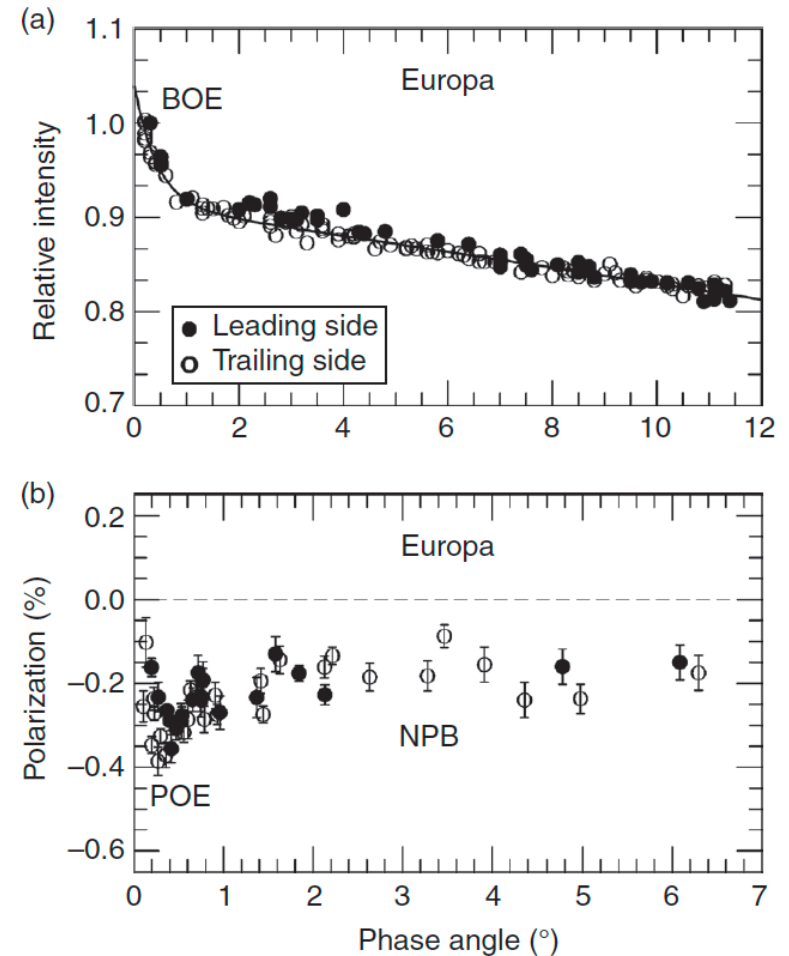


FIGURE 20.5 The brightness (a) and polarization (b) opposition effects for Europa. The filled (open) symbols show polarization for the leading (trailing) hemisphere. The brightness data, taken from Thompson and Lockwood (1992), are fitted according to (Rosenbush *et al.* 2002).

- So-called polarization opposition effects unclear for Io and Ganymede
- What about the flat part of the negative polarization branch, real behavior or systematic error?

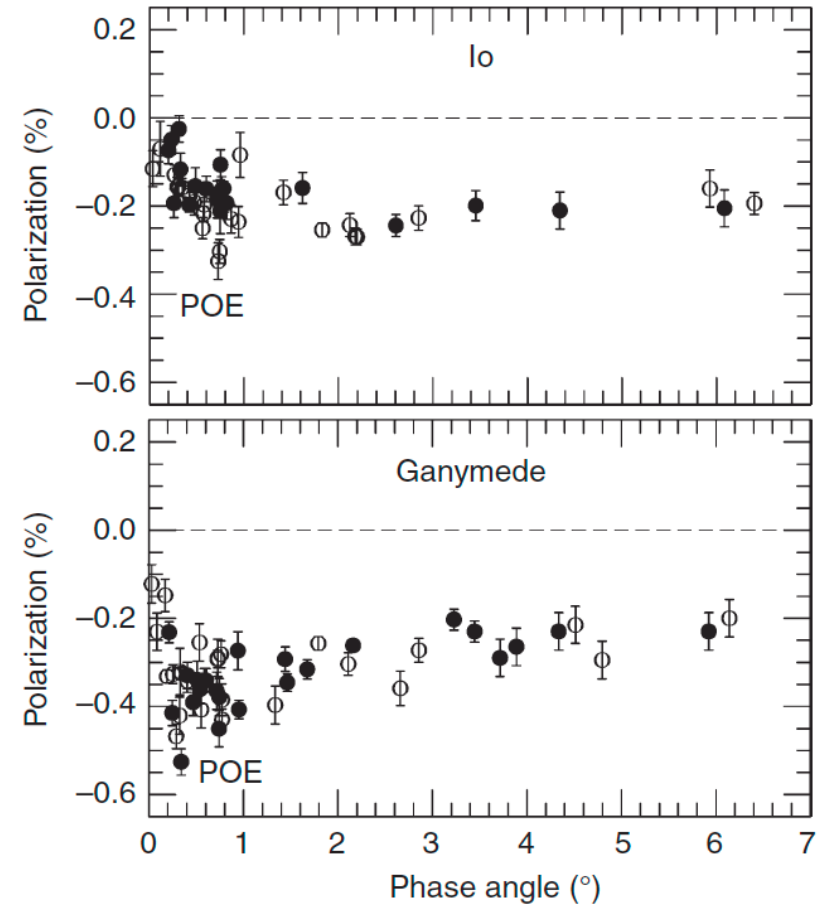


FIGURE 20.6 The POE for Io and Ganymede based on all available measurements of polarization at small phase angles in the V and R filters obtained during the 1988–2014 oppositions (Zaitsev *et al.* 2012b, as well as unpublished data obtained in 2012–2014). The filled (open) symbols show polarization for the leading (trailing) hemisphere.

Polarimetric data of the Galilean moons from space probes

- Rare data at large phase angles obtained by the Galileo and Pioneer 11 missions
- On average, shallow maximum polarizations recorded in accordance with the minimum polarizations

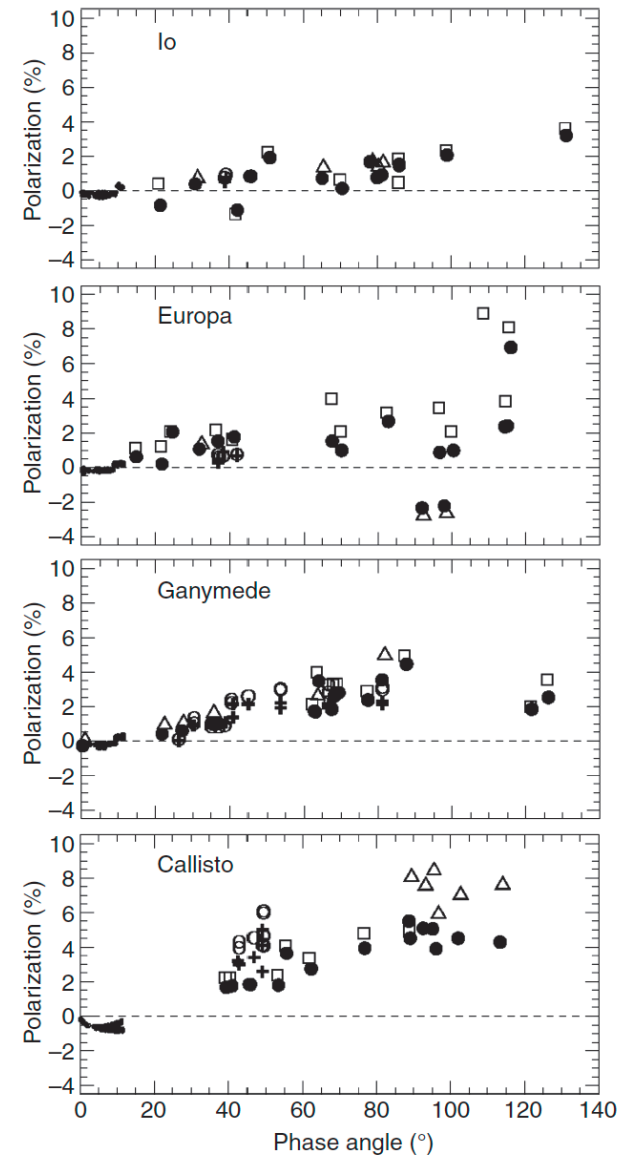


FIGURE 20.7 Measured degree of linear polarization of the Galilean moons obtained from the Earth at phase angles $\alpha \approx 0.2$ – 12° , from the Galileo mission up to 130° (open triangles are measurements in the 410-nm filter; filled circles, 678-nm filter; and open squares, 945-nm filter), and from the Pioneer 11 mission up to 80° (open circles, 450 nm; plus signs, 650 nm). The space data are taken from Martin *et al.* (2000) and Travis *et al.* (2002).

Spectral dependence of polarization for the Galilean satellites

- $|P_{\min}|$ decreases with wavelength in the UV, most for Io and least for Callisto
- $|P_{\min}|$ slightly increases in the red
- Leading and trailing hemispheres show different rates of change (leading show stronger trends in UV)

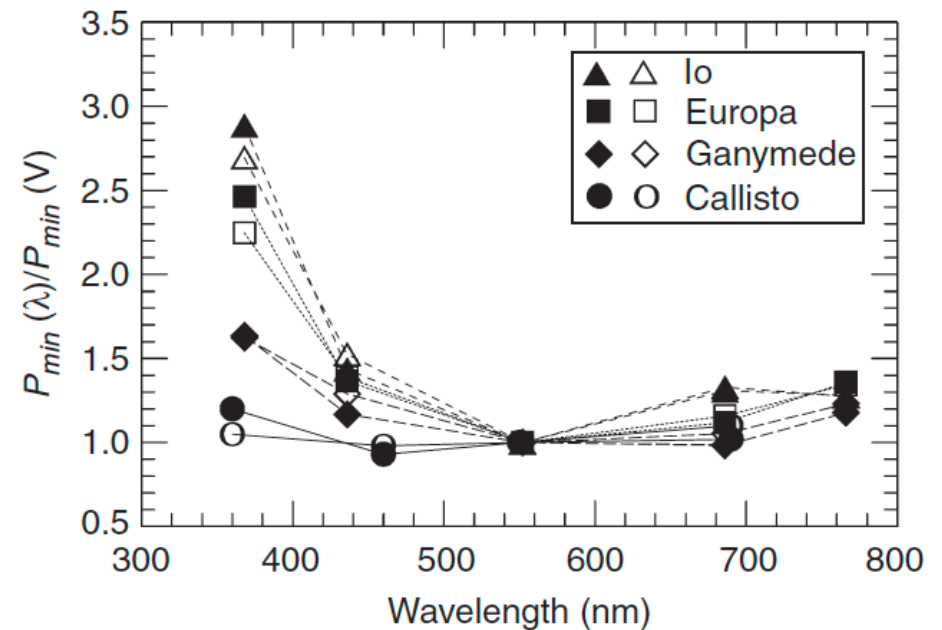


FIGURE 20.8 Spectral dependences of normalized negative polarization for the Galilean satellites. Filled (open) symbols refer to the leading (trailing) hemispheres.

Reproduced from Mishchenko *et al.* (2010) with kind permission of Akademperiodyka of the NAS of Ukraine.

Saturnian system: Enceladus, Dione, Rhea, Iapetus, and Tethys

- Enceladus

- the highest geometric albedo in the Solar System: 1.375 ± 0.008
- steep opposition effect

- Rhea and Dione

- albedos 0.949 ± 0.003 and 0.998 ± 0.004
- Dione shows the greatest albedo dichotomy after Iapetus

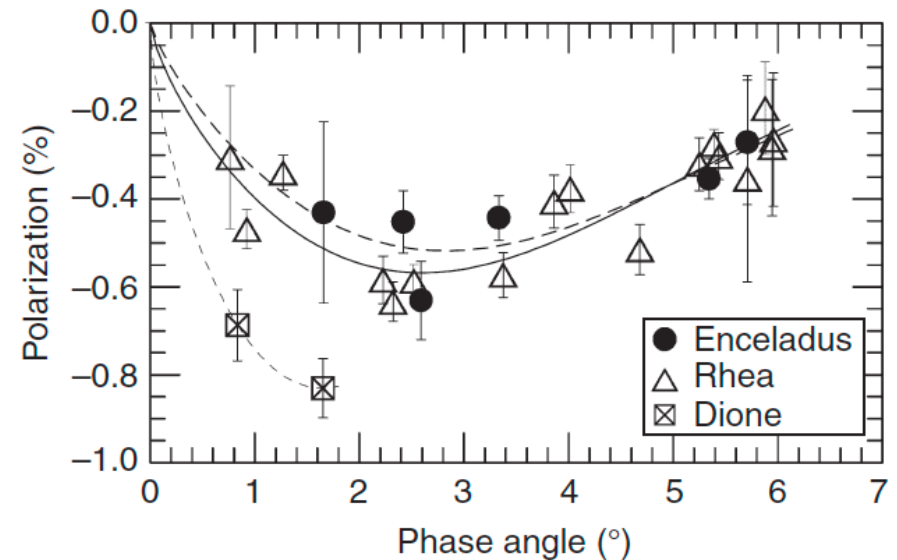


FIG. 20.9 The NPBs for Enceladus, Dione, and Rhea. For Enceladus and Rhea, the observations of the leading and trailing hemispheres are not separated. For Dione, only the trailing side was observed. The curves show the fit to the data; the solid curve is for Rhea, while the dashed curves are for Enceladus and Dione.

Iapetus

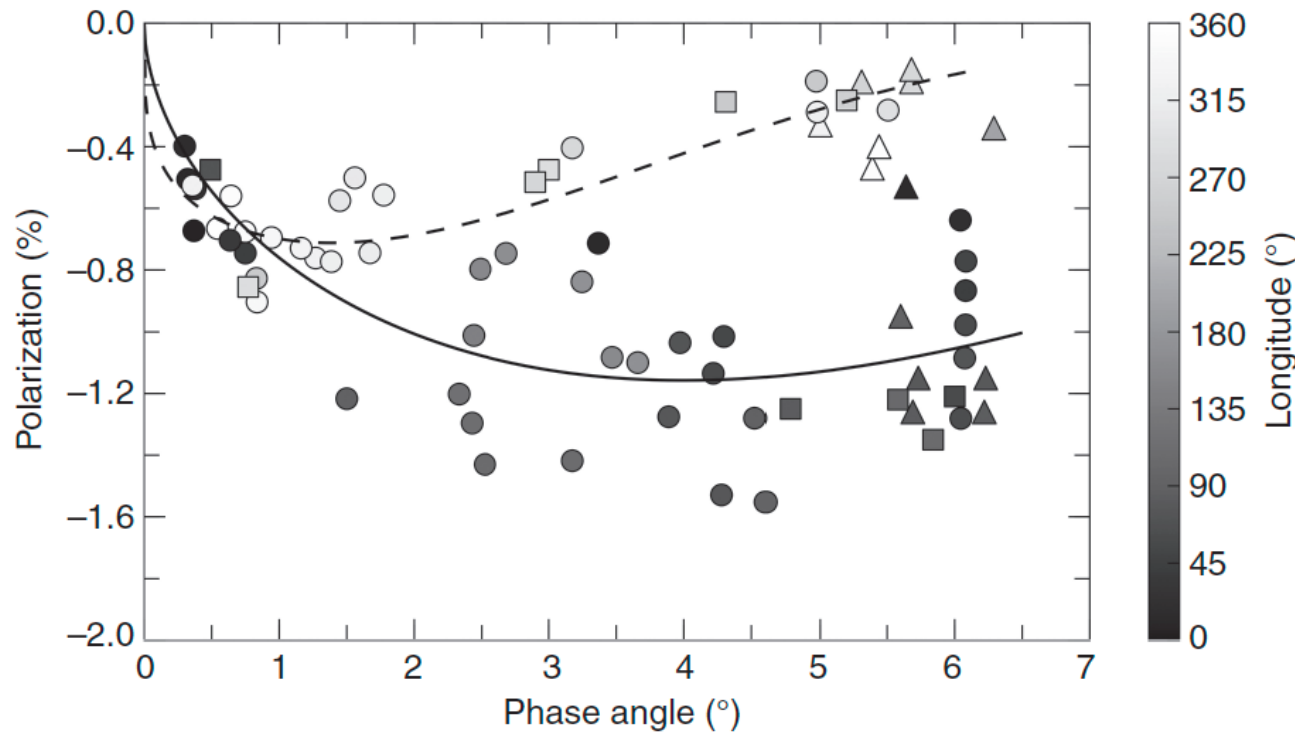


FIGURE 20.10 The observed degree of polarization for Iapetus in the R filter versus phase angle. Longitude is shaded according to the bar on the right-hand side. Circles are data obtained by Rosenbush *et al.* (2002, 2012). Triangles and squares show the polarization data taken from Zellner (1972) and Ejeta *et al.* (2012, 2013a), respectively. The corresponding NPBs represent the best fit for the trailing (open symbols, dashed curve) and leading (filled symbols, solid curve) hemispheres data.

- Intriguing inverse problem!
- Leading (trailing) hemisphere has a geometric albedo of 0.02-0.05 (0.5-0.6)
- How to disentangle the phase curves of the different hemispheres?

- First RT-CB modeling carried out with a two-component Rayleigh model
- Improvements could well be accomplished!

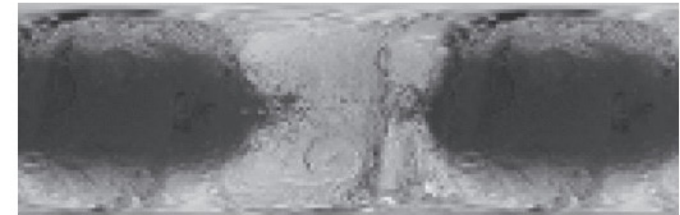
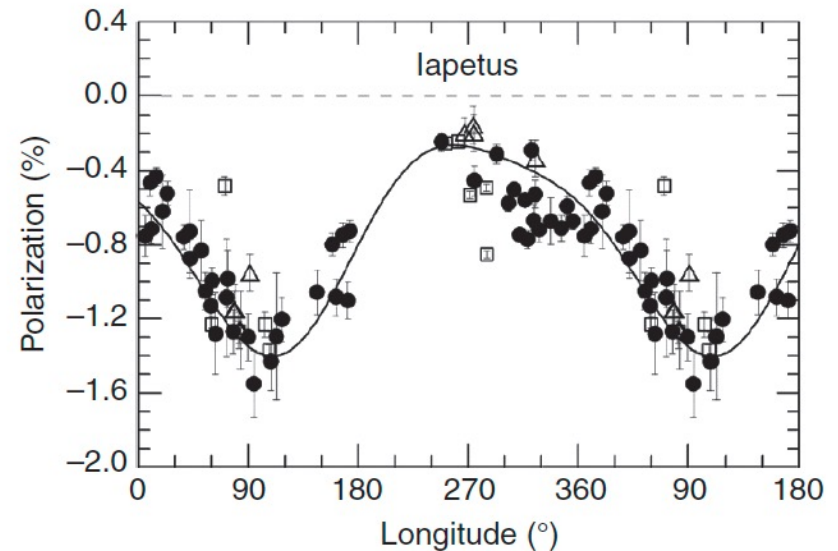


FIGURE 20.11 The observed LDP for Iapetus in the R filter (top panel) and the albedo distribution on the surface of Iapetus (bottom panel). Filled circles: Rosenbush *et al.* (2002, 2012); open triangles: Zellner (1972); open squares: Ejeta *et al.* (2012, 2013a). For continuity, in the upper panel the range $0 < L < 180^\circ$ is repeated on the right-hand side. The map of the albedo distribution in an equirectangular projection corresponds in longitude to the upper panel.

The map is derived from a mosaic of Cassini images (<http://laps.noaa.gov/albers/sos/saturn/iapetus/>, 2008); credit S. Albers, reproduced with permission.

Uranian system: Ariel, Umbriel, Titania, and Oberon

- All show pronounced opposition effects
- The polarization phase curves do not show steep surges (cf. S-type asteroids)
- Spectral dependences confirmed to differ fundamentally from those of Jovian and Saturnian satellites

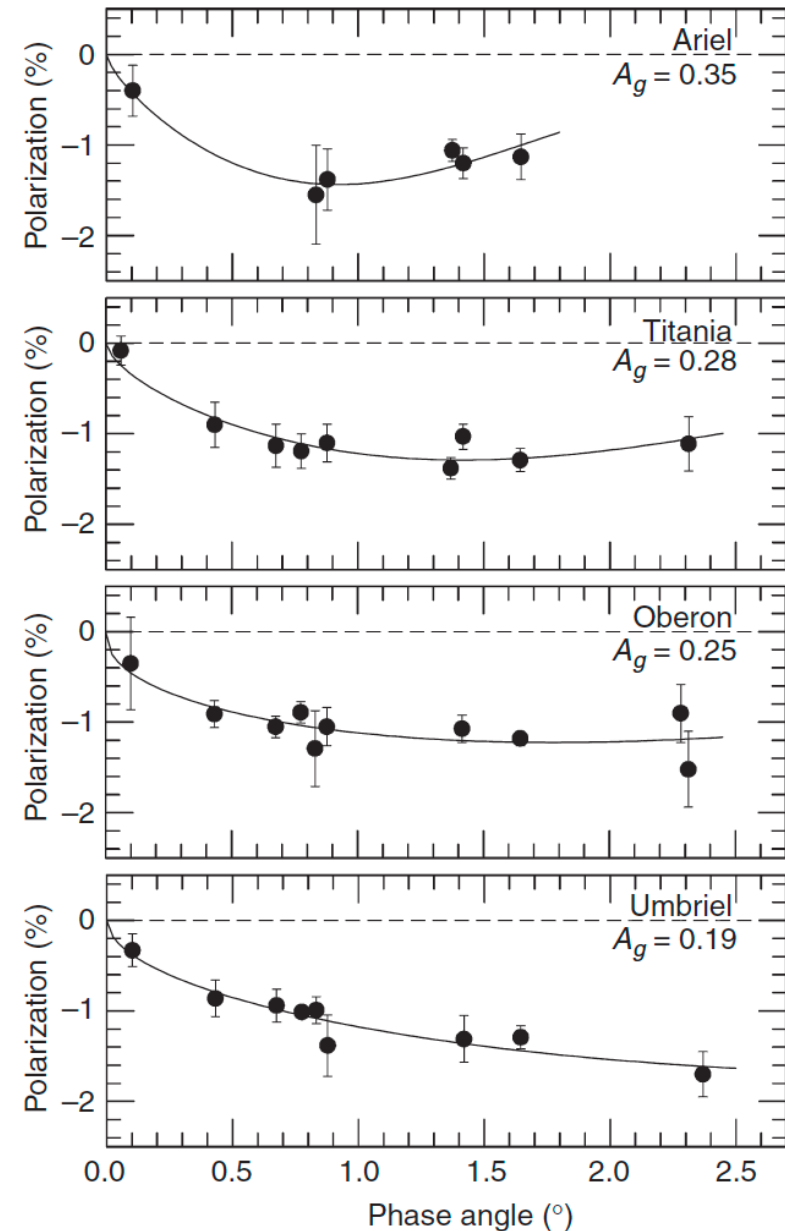
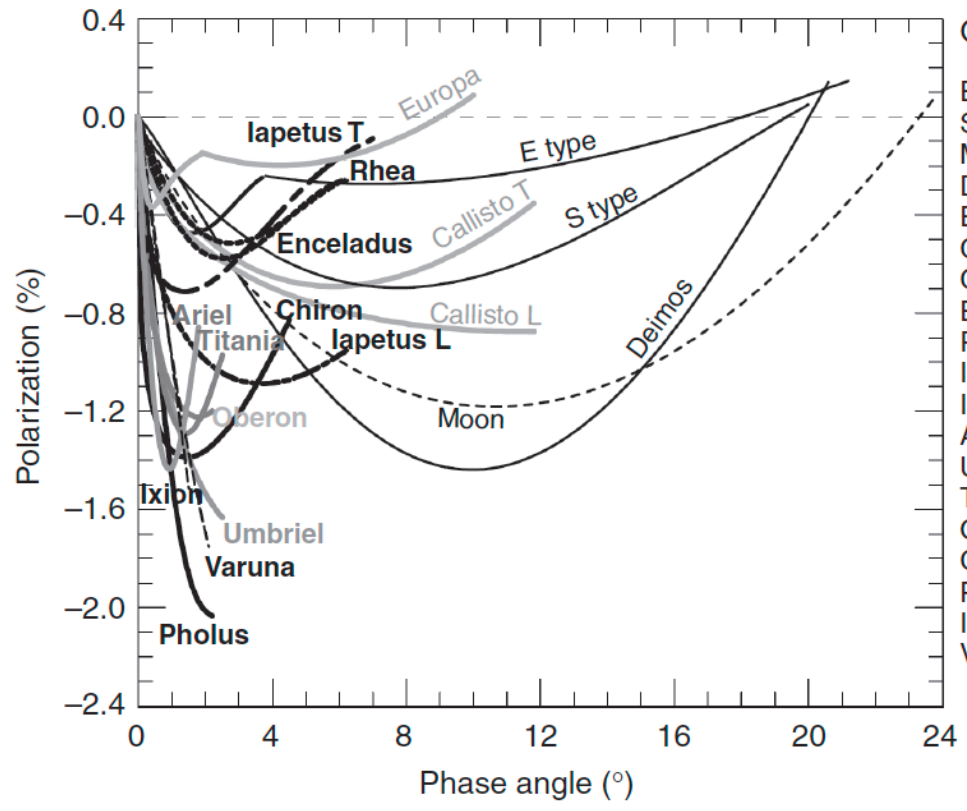


FIGURE 20.12 Phase-angle dependences of polarization for the major moons of Uranus. The curves represent the fit to the data.

Final notes on polarization by satellites



Object	A_g
E type	0.50
S type	0.23
Moon	0.12
Deimos	0.08
Europa	0.68
Callisto T	0.19
Callisto L	0.19
Enceladus	1.38
Rhea	0.95
Iapetus T	0.5
Iapetus L	0.04
Ariel	0.35
Umbriel	0.19
Titania	0.28
Oberon	0.25
Chiron	0.08
Pholus	0.08
Ixion	0.12
Varuna	0.07

FIGURE 20.13 Comparison of polarization–phase curves for different types of objects: terrestrial (Moon), Martian (Deimos), Jovian (Europa, Callisto), Saturnian (Enceladus, Rhea, Iapetus), and Uranian (Ariel, Titania, Oberon, Umbriel) moons; E- and S-type asteroids; Centaurs (Chiron, Pholus); and TNOs (Ixion, Varuna). The geometric albedos of these objects are tabulated on the right-hand side. For illustration, a second local minimum of polarization near opposition is only shown for the Jovian satellite Europa and the E-type asteroids. See references for data in Rosenbush and Mishchenko (2011), Bagnulo *et al.* (2011), Belskaya *et al.* (2010), and Johnston (2013).

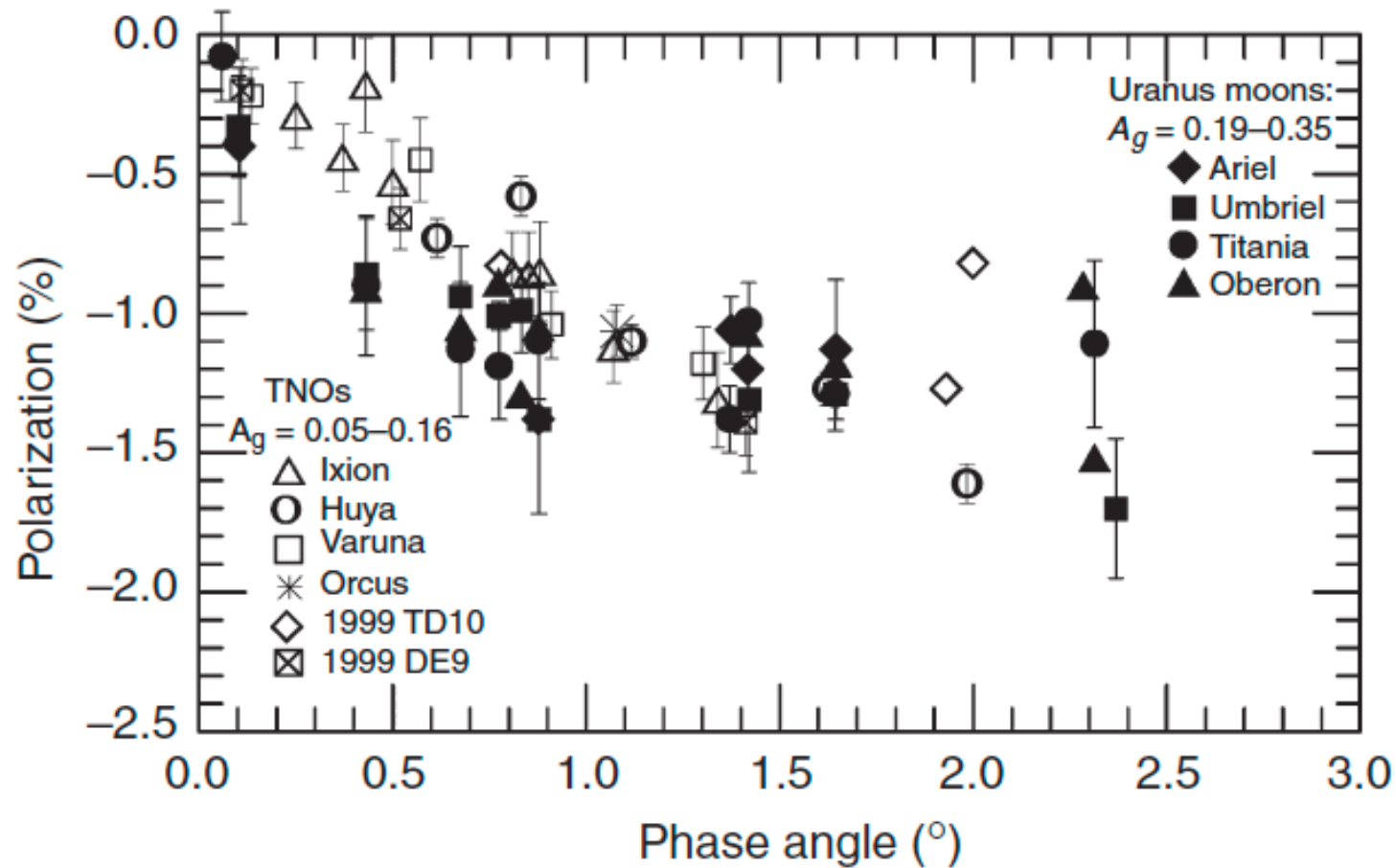


FIGURE 20.14 Comparison of the polarization of the Uranian moons (dark symbols) and TNOs (open symbols).

Data for TNOs are taken from Bagnulo *et al.* (2011) and Belskaya *et al.* (2012).

Example: Jovian moon Europa

**Kiselev et al.,
unpublished**

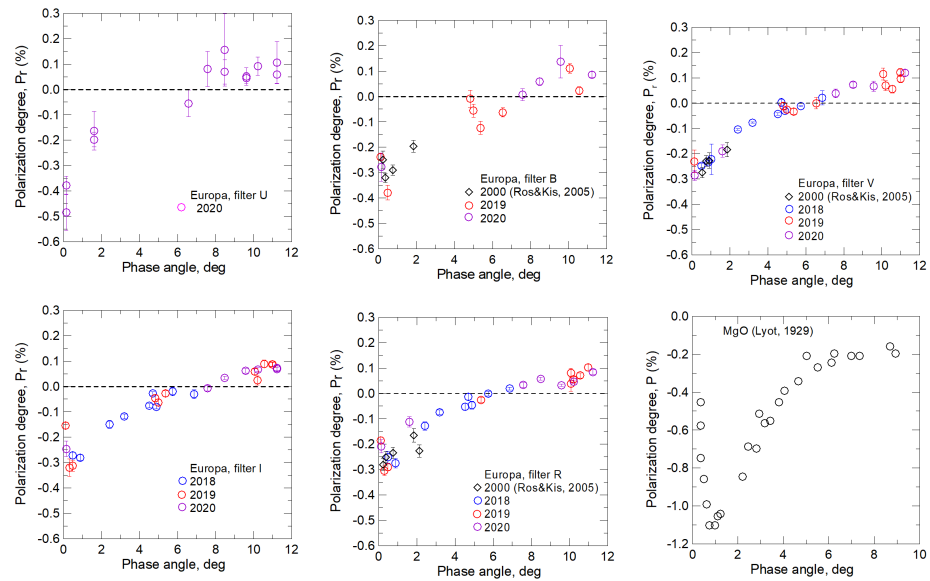


Fig. 2. Phase-angle polarization dependences for Jupiter's satellite Europa in the *UBVR* filters, obtained in 2018–2020 (open circles) and in 2000 (Rosenbush and Kiselev, 2005) (diamonds). For comparison (bottom row, right panel), the results of laboratory measurements of the polarization of MgO are presented (adopted from the paper by Lyot, 1929).

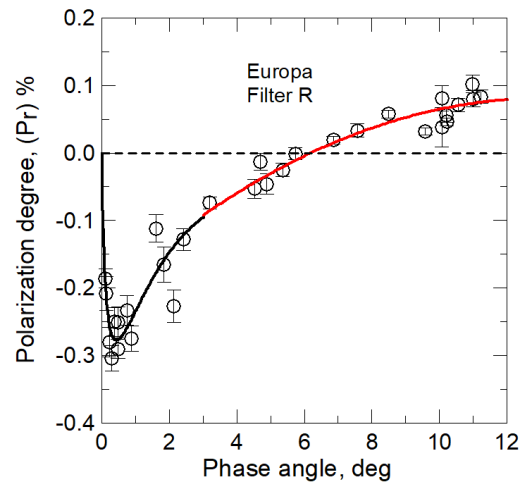


Fig. 3. The fits of Europa's data in the *R* filter taken from Table 4 and Rosenbush&Kiselev 2005). The black curve is an approximation of data in the phase angle interval $\approx(0^\circ - 3^\circ)$ with expression (7), while the red curve is the fitting of data in the phase angle interval $\approx(3^\circ - 12^\circ)$ with a second-degree polynomial.

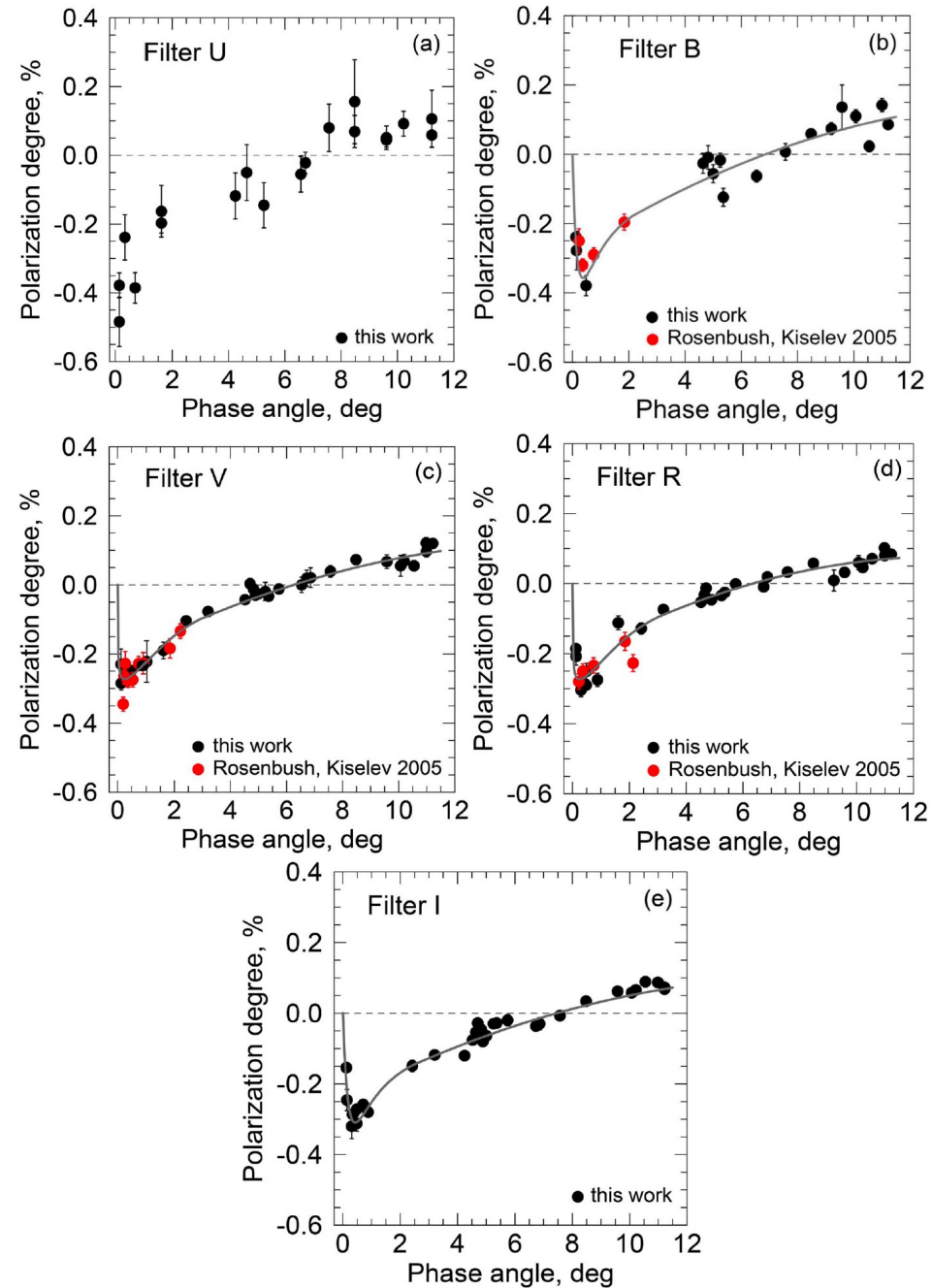
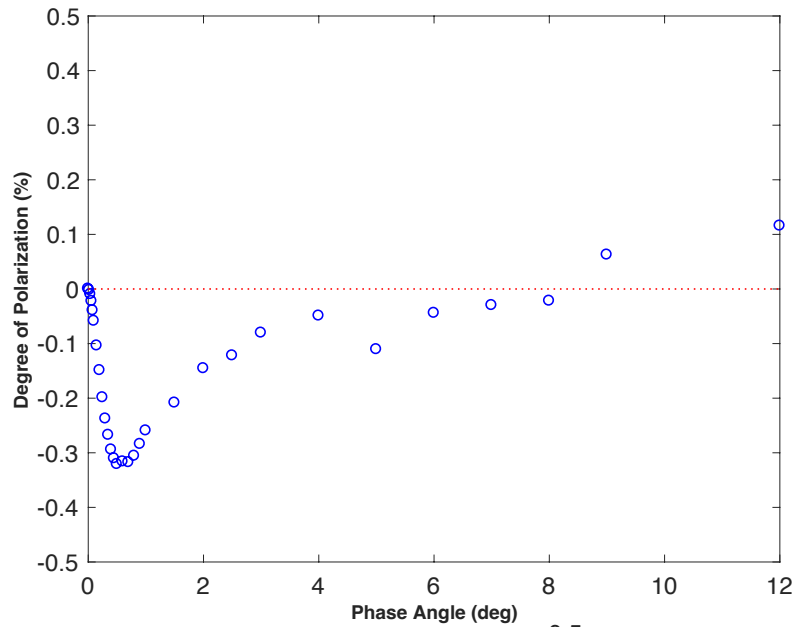
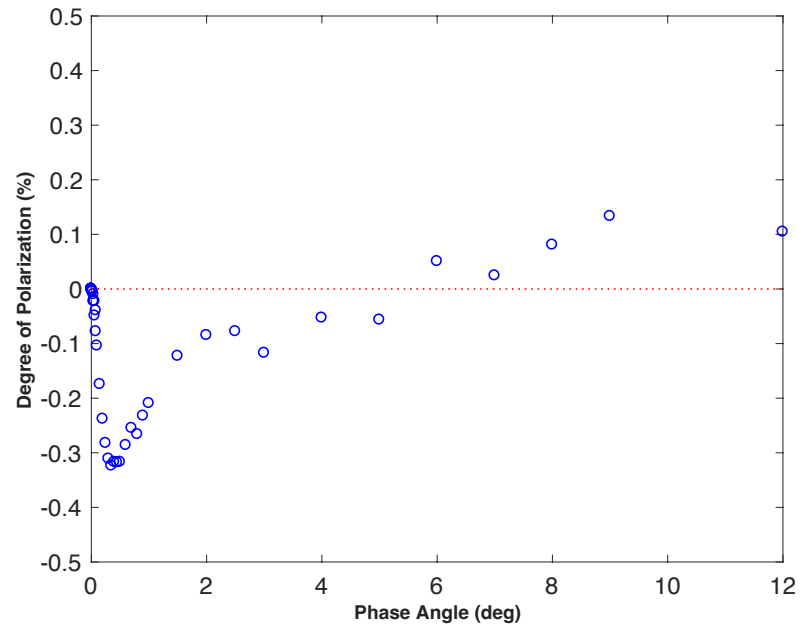


Figure 2. The phase-angle dependence of polarization for Europa in the *UBVRI* filters obtained in 2018–2021 (black circles) and in 2000 (Rosenbush & Kiselev 2005; red circles). The fit to the *BVRI* data showed by the solid curve consists of two parts: an approximation of data within the range of phase angles from 0° to $\sim 3^\circ$ and in the phase-angle range from approximately 3° to 12° using polynomials of the third and second degree, respectively.

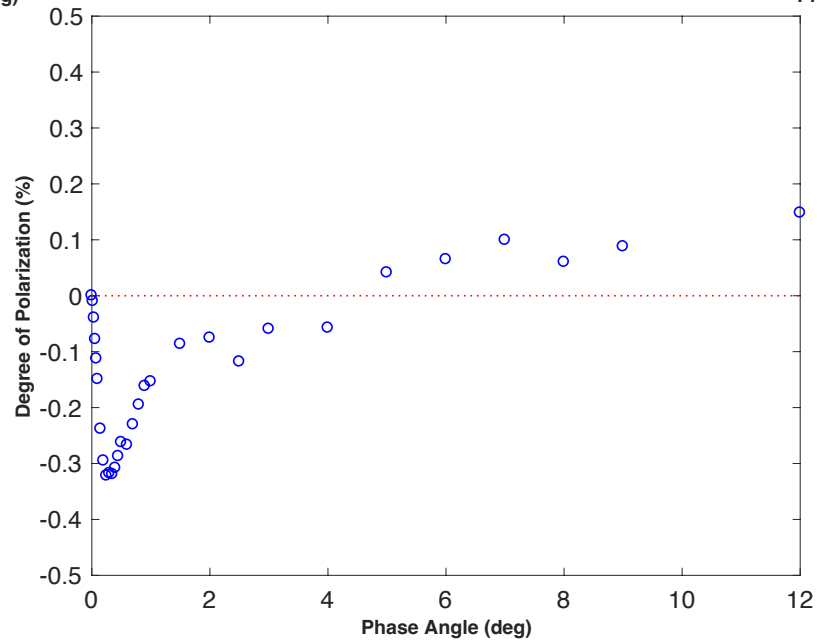
kl = 100



kl = 150



kl = 200



$\omega = 0.984$
 $P_{\max} = 0.08$
 $g = 0.6$
 $g_1 = 0.8$
 $g_2 = -0.1$
($p = 0.67-0.68$)

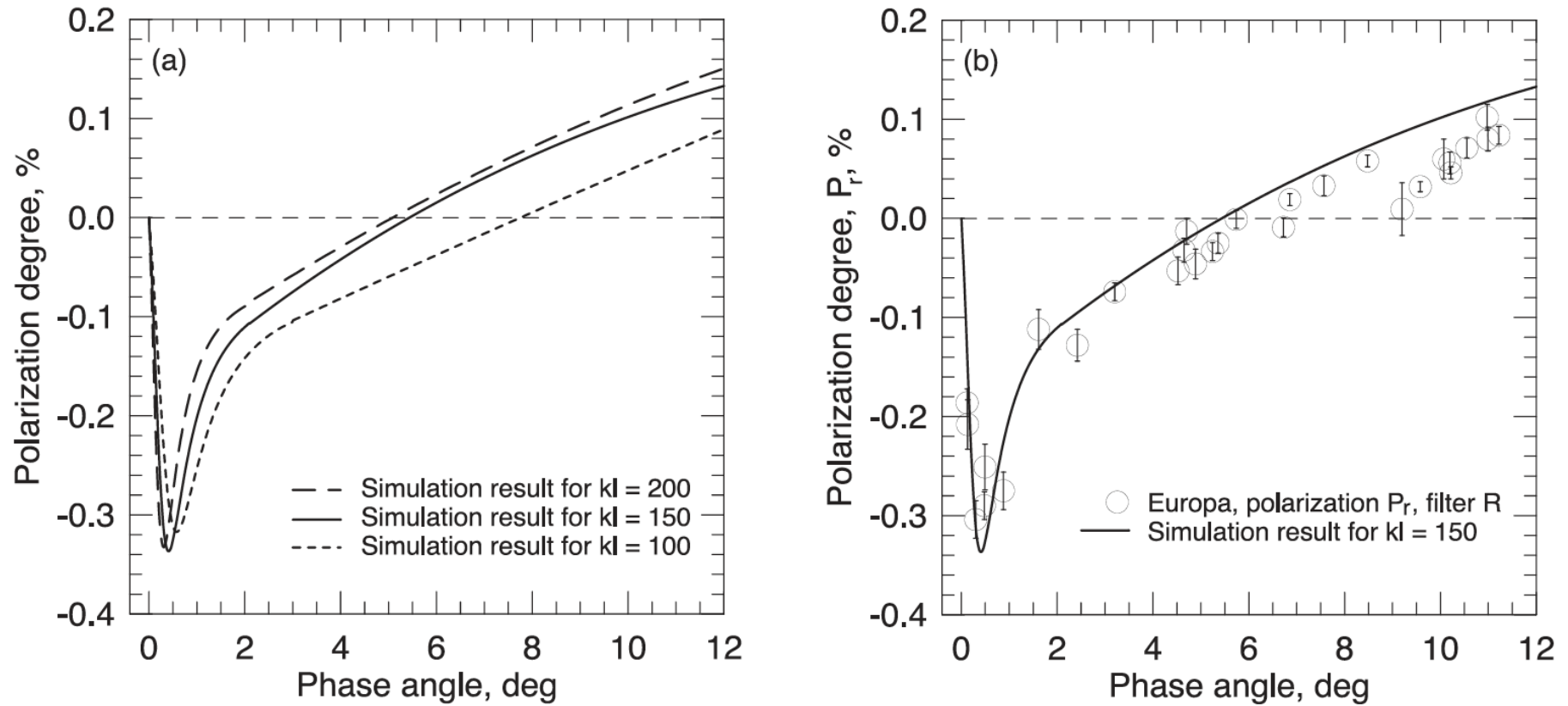


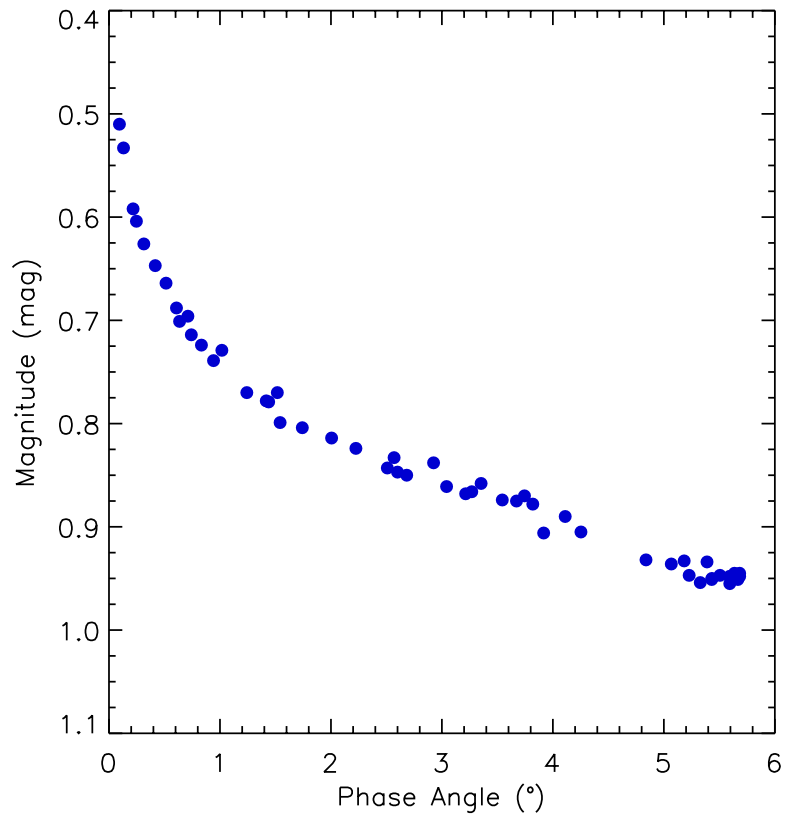
Figure 4. (a) Shifting the inversion point with increase of kl . (b) The best fit to the observational data in the R filter.

Table 3
Physical and Model Parameters

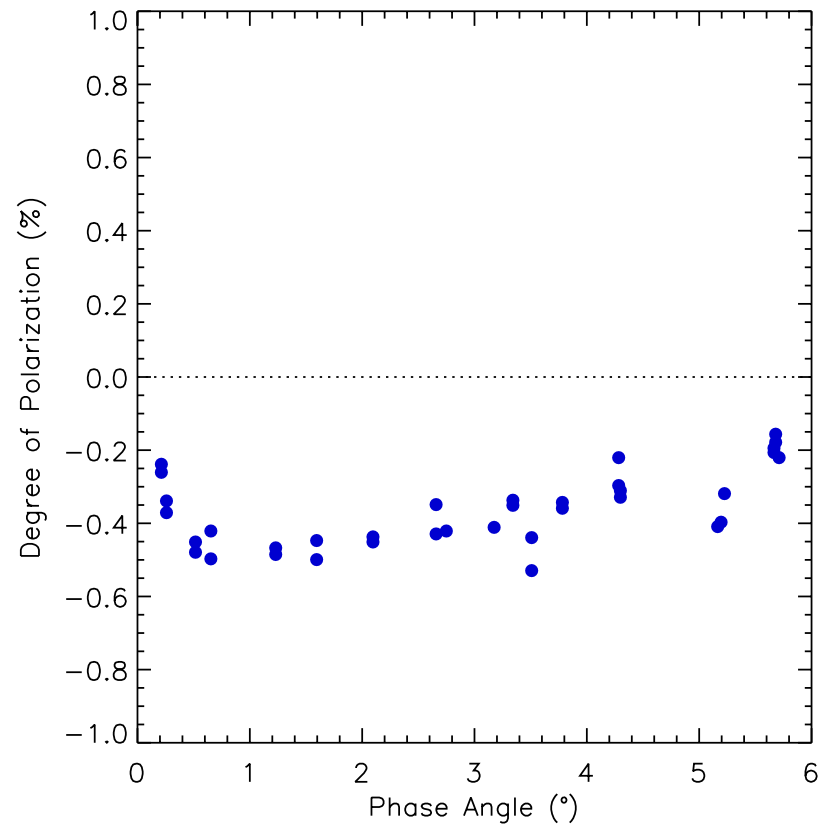
Parameters (Symbol)	Value
Single-scattering albedo (ω)	0.985
Parameters of double Henyey–Greenstein function (g, g_1, g_2)	$g = 0.6, g_1 = 0.8, g_2 = -0.1$
Maximum of polarization degree for the case of single scattering (p_{\max})	0.08
Number of rays used in the Monte Carlo modeling (N)	10^7
Mean free path lengths (kl)	100, 150, 200

Saturn's Rings

Photometry



Polarimetry



Conclusion and perspectives

- RT-CB modeling highly challenging due to the high geometric albedos
- Recent modeling quite successful for Europa
- Modeling could well be improved by incorporating more realistic modeling of single scattering
- Laboratory measurements of single scattering extremely challenging for ices!
- Additional observations called for using large telescopes across the spectrum from UV to NIR
- Accuracy of the observations to be improved
- Why are the new Europa polarimetric observations different from the older ones?

Light-scattering experiment: Rainbows @ home

- Equipment
 - Source of light, e.g., headlamp
 - Circular-cylindrical glass bottle, e.g., water bottle
 - Detector screen
- Measurement
 - Fill in the bottle with water
 - Illuminate horizontally with light source
 - Detect rainbows on the screen
- Question
 - Rainbow angles for water or for glass?
 - Provide argumentation